Learning to Localize Itself
- Vision-Motor Association for Legged Robot -

T. Miyashita, S. Doi, M. Asada, & K. Hosoda

Adaptive Machine Systems, Graduate School of Engineering
Osaka University, Suita, Osaka 565-0871, Japan
miyasita@er.ams.eng.osaka-u,ac.jp

ABSTRACT

This paper presents a method that acquires a vision-motor association for a legged robot as a bottom-up technique for self localization by action based perception categorization. By the method, the legged robot can move to the position where it can capture desired view. The validity of the method is shown by a preliminary experiment, and future work is given.

1 INTRODUCTION

In the RoboCup Initiative [1], each player has to make quick decisions in any game situations to behave reactively and rationally. In order to realize such capabilities, self-localization has been regarded as one of the main issues. A typical solution is to reconstruct a global view of the entire field and then to calculate the self position from ideothetic and/or allothetic information such as landmarks and dead-reckoning. In the case of the wheeled robots, Uchida et. al. used dead-reckoning and a three-dimensional map [2], and Olson used landmarks and an environmental model [3]. Veloso also realized localization of the legged robot by using landmarks and Bayesian localization procedure [4]. These approaches, however, need explicit knowledge on proprioception and exteroception such as kinematic parameters of the robot and the internal / external camera parameters. These should be carefully calibrated in advance by the designer. This process is often tedious and time-consuming. From a viewpoint of cognitive robotics, how to associate robot proprioception with its exteroception is a more interesting issue, especially in the case of legged robots to which dead-reckoning is more difficult to apply than to wheeled robots.

In this paper, we propose a method of action based perception categorization for a legged robot to move to any destination in the environment. Once the robot acquires the relationship between actions and the changes of the view, it can generate the motion with respect to the observed environment. By utilizing the relationship, it achieve the desired position by feeding back the difference between the goal view and the current one. First, the legged robot learns to walk based on visual cues given by a teacher [5]. This can be regarded as a kind of adaptive visual servoing [6]. During this process, the robot observes its walking motion patterns and the changes of the view. Next, the robot classifies the walking motion patterns and the changes of the view separately, and acquires the relationship between them. Consequently, it can move to any position based on the relationship and the adaptive servomechanism.

The rest of this article is structured as follows. First, we explain system requirements for our method. Next, we present the method of categorizing perception and acquiring the relationship between action and perception. Then, we show a preliminary experimental results in a real environment to verify the validity of the motion pattern extraction. Finally, the future work is given.

2 THE SYSTEM AND BASIC BEHAVIORS

2.1 A Legged Robot

We use a following quadruped robot as a legged robot which has:

- four legs, each of which has three degrees of freedom,
- four force sensors attached to each foot for calculating a zero moment point,
- an uncalibrated TV camera, and
- twelve joint angle sensors.

2.2 Reflective Walk Based on Visual Cues

We present a reflective walk of a quadruped robot based on reflections to realize an adaptive walk in a dynamic environment. The combination of reflections, a vision-cued swaying reflection and a reflective gait, makes the robot walk reflectively, without programming the exact motion of each joint of the legs. Figure 1 (a) and (b) show outlines of such two reflections.

The former reflection, the vision-cued swaying reflection, makes the robot sway to stabilize a visual target at the desired position in the image. A stimulus to sway is a motion of the visual target. The latter one, the reflective gait, makes it change step to avoid falling down. A stimulus of it is a motion of the zero moment point (here after, ZMP).

By combining them, the robot sways the body attempting at tracking the visual target, and changes step if it becomes off balance. Consequently, the walking motion emerges according to the target motion.

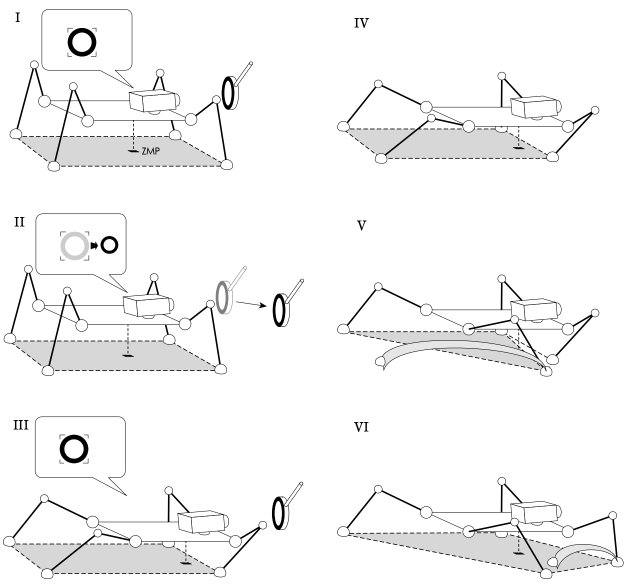

(a) A vision-cued swaying reflection

(b) A reflective gait

Figure 1: Outlines of two reflections

2.2.1 Vision-Cued Swaying Reflection We apply the adaptive visual servoing to the legged robot in order to realize the vision-cued swaying reflection. Assume that the robot can observe the visual target, and obtain its kinetic parameters.

Let Σ_R, ${}^R\boldsymbol{p}$, ${}^R\boldsymbol{r}_i$ and $\boldsymbol{l}$ denote a robot coordinate frame fixed to the robot body, a position vector of a camera attached to the robot with respect to Σ_R, the i-th foot position vector w. r. t. Σ_R and a stance vector consists of distances between feet, respectively. Defining ${}^R\boldsymbol{r}$ by

$$ {}^R\boldsymbol{r} \triangleq \left[{}^R\boldsymbol{r}_1^T\,{}^R\boldsymbol{r}_2^T \cdots {}^R\boldsymbol{r}_n^T\right]^T \quad , \tag{1} $$

we can obtain two velocity relations,

$$ \dot{\boldsymbol{l}} = \boldsymbol{J}_{lr}\,{}^R\dot{\boldsymbol{r}} \quad , \tag{2} $$

$$ {}^R\dot{\boldsymbol{p}} = \boldsymbol{J}_{pr}\,{}^R\dot{\boldsymbol{r}} \quad , \tag{3} $$

where $\boldsymbol{J}_{lr} = \partial\boldsymbol{l}/\partial^R\boldsymbol{r}^T$ and $\boldsymbol{J}_{pr} = \partial\boldsymbol{p}/\partial^R\boldsymbol{r}^T$, respectively.

Let $\boldsymbol{x}$ be a vector of the image features. Assume that the visual target is moving so slowly that one can neglect the velocity of the target comparing to the velocity of the robot. If the feet of the robot are fixed on the ground, we can obtain a velocity relation,

$$ \dot{\boldsymbol{x}} = \boldsymbol{J}_{xp}\,{}^R\dot{\boldsymbol{p}} = \boldsymbol{J}_{xp}\boldsymbol{J}_{pr}^{+}\,{}^R\dot{\boldsymbol{r}} = \boldsymbol{J}_{xr}\,{}^R\dot{\boldsymbol{r}}. \tag{4} $$

From eqs.(2) and (4), visual servoing controller for the vision-cued swaying reflection, which makes the image feature vector $\boldsymbol{x}$ converge to a given desired trajectory $\boldsymbol{x}_d$ under a control of the feet distance vector $\boldsymbol{l}$ constant to fix the feet on the ground, can be derived as

$$ \begin{aligned} \boldsymbol{u}_r = \; & \boldsymbol{J}_{lr}^{+}\boldsymbol{K}_l\left(\boldsymbol{l}_d - \boldsymbol{l}\right) \\ & + \left(\boldsymbol{I} - \boldsymbol{J}_{lr}^{+}\boldsymbol{J}_{lr}\right)\left\{\boldsymbol{J}_{xr}\left(\boldsymbol{I} - \boldsymbol{J}_{lr}^{+}\boldsymbol{J}_{lr}\right)\right\}^{+} \\ & \left\{\boldsymbol{K}_x\left(\boldsymbol{x}_d - \boldsymbol{x}\right) - \boldsymbol{J}_{xr}\boldsymbol{J}_{lr}^{+}\boldsymbol{K}_l\left(\boldsymbol{l}_d - \boldsymbol{l}\right)\right\}, \end{aligned} \tag{5} $$

where $\boldsymbol{u}_r$, $\boldsymbol{K}_l$ and $\boldsymbol{K}_x$ denote a control input vector and gain matrices, respectively.

In the controller (5), we can obtain the Jacobian matrix $\boldsymbol{J}_{lr}$ from kinematic parameters of the robot. But, since the matrix $\boldsymbol{J}_{xr}$ consists not only of the kinematic parameters that are known, but also of intrinsic and extrinsic camera parameters and of the parameters of the environment, we need to estimate the matrix $\widehat{\boldsymbol{J}}_{xr}$ that satisfies eq.(4) by correcting $\boldsymbol{r}$ and $\boldsymbol{x}$. We utilize a least squares method to identify the non-linear system in the discrete time domain:

$$ \begin{aligned} & \{\widehat{\boldsymbol{j}}_i(k+1) - \widehat{\boldsymbol{j}}_i(k)\} = \\ & \frac{\{\boldsymbol{x}(k+1) - \boldsymbol{x}(k) - \widehat{\boldsymbol{J}}_{xr}(k)\boldsymbol{u}_r(k)\}_i}{\rho_i + \boldsymbol{u}_r(k)^T\boldsymbol{W}_{(i,k)}\boldsymbol{u}_r(k)}\boldsymbol{W}_{(i,k)}\boldsymbol{u}_r(k) \end{aligned} \tag{6} $$

where $\widehat{\boldsymbol{J}}_{xr}(k)$, $\widehat{\boldsymbol{j}}_i(k)$, $\boldsymbol{u}(k)(=\Delta T\dot{\boldsymbol{r}})$, ρ_i and $\boldsymbol{W}_i(k)$ denote a constant Jacobian matrix, its i-th row vector, a control input vector in the k-th step during sampling interval ΔT, an appropriate positive constant and a weighting matrix, respectively. Using the estimated matrix $\widehat{\boldsymbol{J}}_{xr}$, we can rewrite the controller (5) as

$$ \begin{aligned} \boldsymbol{u}_r = \; & \boldsymbol{J}_{lr}^{+}\boldsymbol{K}_l\left(\boldsymbol{l}_d - \boldsymbol{l}\right) \\ & + \left(\boldsymbol{I} - \boldsymbol{J}_{lr}^{+}\boldsymbol{J}_{lr}\right)\left\{\widehat{\boldsymbol{J}}_{xr}\left(\boldsymbol{I} - \boldsymbol{J}_{lr}^{+}\boldsymbol{J}_{lr}\right)\right\}^{+} \\ & \left\{\boldsymbol{K}_x\left(\boldsymbol{x}_d - \boldsymbol{x}\right) - \widehat{\boldsymbol{J}}_{xr}\boldsymbol{J}_{lr}^{+}\boldsymbol{K}_l\left(\boldsymbol{l}_d - \boldsymbol{l}\right)\right\}. \end{aligned} \tag{7} $$

2.2.2 Reflective Gait We use a stability margin, which is the shortest distance between the zero moment point (here after, ZMP) and a side of the supporting leg polygon, as a measure of the stability of the legged robot (see Figure 2). If the robot sways the body due to visual servoing, the stability margin becomes small as shown in Figure 2(b). To increase the margin in such a case, it has to lift a leg up and move it, which we call "target leg" in the following.

In Figure 2(b), candidates for the target leg are indicated as "×". They can not be lifted up because ZMP is always inside two supporting leg triangles including the both target legs. In such a case, therefore, the reflective gait control lifts one of the other legs so as to make the target leg to be lifted (see Figure 3(a)), and moves the target leg to increase the stability margin (see Figure 3).

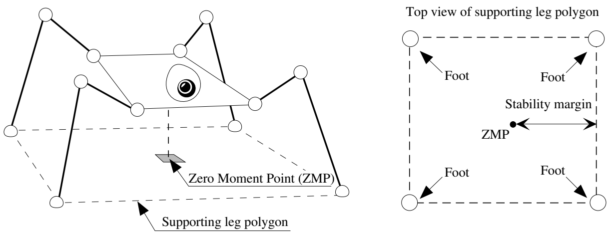

(a) a stable pose

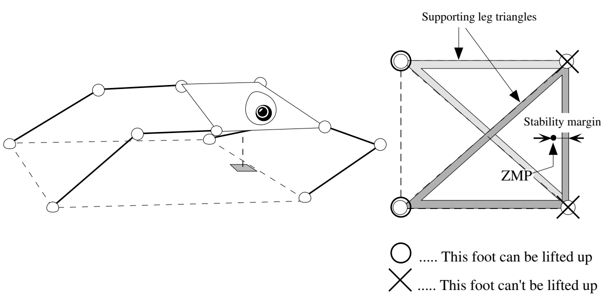

(b) an unstable pose

Figure 2: The relationship between the stability margin and the feet

3 ACTION BASED PERCEPTION CATEGORIZATION

3.1 Motion Pattern Extraction

The walking motion patterns of the legged robot can be described in terms of time series data of all joint angular velocities. It is, however, difficult to memorize and utilize such data because of their huge size.

In order to realize compact description for them, we segment such spatiotemporal data into each walking cycle under an assumption that the walking motion patterns are periodic. Then, we compress them using wavelet transform [7], which localizes a function, called a mother wavelet, both in space and scaling. We use Daubechies N=6 as the mother wavelet (see figure 4) and remove high and law frequencies from the wavelet coefficients as noise.

After the transformation, we classify the coefficients based on the action similarity by using centroid method which is one of the hierarchical cluster analysis. The objects to be clustered are the group of features of the coefficients which are the largest time differential value and its position in a walking cycle (see figure 5).

3.2 Perception Categorization

Unlike wheeled robots, the motions of actuators of legged robots do not correspond directly to the motion with respect to the observed environment. Hence to acquire such relationship is necessary to achieve the desired position in the environment. In this method, we use an optical flow taken from a TV camera on the legged robot which show the changes of the view owing to its action and also describe the motion with respect to the observed environment.

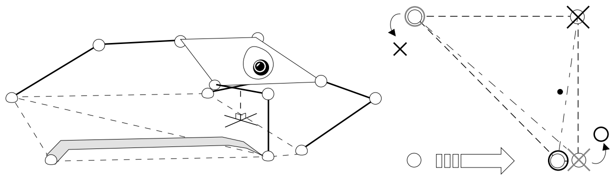

(a) Making the leg a lifted leg

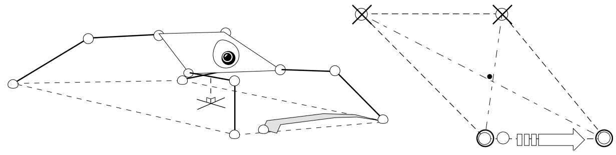

(b) Moving the lifted leg

Figure 3: The reflective gait

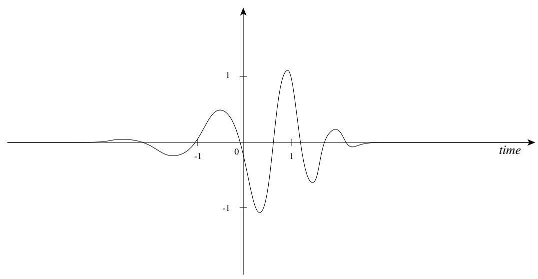

Figure 4: The mother wavelet (Daubechies N=6)

First, we segment the image plane into four regions and calculate a vector which denote the spatial average of the whole optical flow in each region (see Figure 6) to reduce the dependency on the specific position in the environment. Next, we calculate the time averages of such vectors during a walking cycle and obtain a vector consists of them. Finally, we classify the obtained vectors by using the centroid method, and acquire the flow pattern which denote the change of the view during the cycle.

3.3 Vision-Motor Association

The robot can acquire a simple map which denotes the relationship between the clusters of the action and the flow patterns described above. If the flow patterns are sufficient to represent the robot motion with respect to the observed environment, the robot can move to

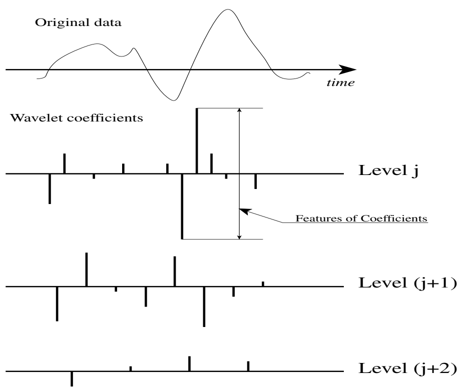

Figure 5: The feature point of the wavelet coefficients

anywhere in the environment. For example, if we give the robot the view of landmarks from the goal position, the robot selects the flow pattern to move the position of the landmarks in the image plane to the goal, and generates the corresponding walking motion pattern by the map. Consequently, it achieves the goal by feeding back the difference between the goal view and the current one.

4 EXPERIMENTS

4.1 Experimental Systems

In Figure 7, a legged robot TITAN-VIII [8] and its controller used for the experiment are shown. The legged robot is equipped with one camera (EVI-310, SONY). The image from the camera is sent to a tracking unit (TRV-CPD6, Fujitsu) equipped with a high-speed correlation processor [9]. Before starting an experiment, we give four 16[pixel] $\times$ 16[pixel] patterns (called reference patterns) to be tracked. During the experiment the unit feeds coordinates where the correlation coefficient is the highest with respect to the reference patterns to the host computer G6-200 (Gateway2000, CPU:Intel Pentium Pro 200MHz) through a PCI-bus link in real-time (33[ms]). Each joint of the legged robot is equipped with a potentiometer to observe its joint angle. Each foot is also equipped with a force sensor to observe its foot force and to estimate the position of ZMP. The observed joint angles and the foot forces are sent to the computer through an A/D converter board (RIF-01, Fujitsu). The computer calculates the desired joint velocities and sends the commands to the velocity controllers of joints through a D/A converter board (RIF-01, Fujitsu). A hand cart is used to move three target marks.

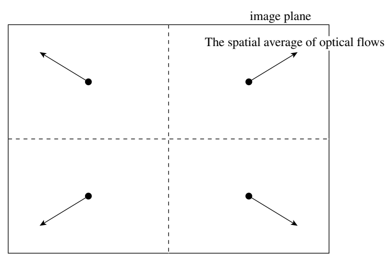

Figure 6: The four regions and a coarse flow (average of the whole flow)

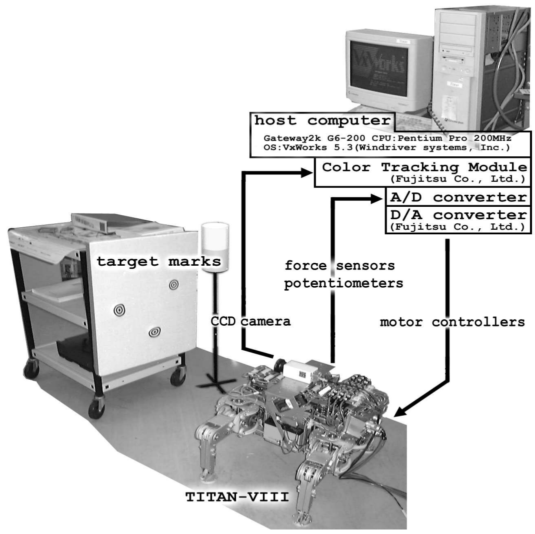

Figure 7: Experimental systems

4.2 Experimental Results

We show preliminary experimental results of the motion pattern extraction for the legged robot. In this experiment, the visual targets were moved to forward and rightward of the robot. Figures 8 (a) and (b) show how the robot walks reflectively.

During walking, the robot memorizes the time series data of the angular velocities of all joints, and segments them into each walking cycle (C_i) which can be observed by foot force sensors. In this case, the robot memorized ten walking cycles ($C_{1\cdots10}$). The motion of the robot during C_1 to C_5 were forward and the others were rightward. In a part of figures 8 (a) show the motion during C_1, and in a part of figures 8 (b) show the motion during C_6. Figures 9 (a), (b), (c), (d), (e), and (f) show the time series data of right-foreleg during C_1 and C_3. Figures 10 (a), (b), (c), (d), (e), and (f) also show the data during C_6 and C_8.

Next, the robot compresses the data based on wavelet transform, and classifies them by using the centroid method. Figures 11 show the wavelet coefficients of the first joint during C_1 and C_6. A result of classification is shown in figure 12. This figure indicates that the robot motion can be clearly classified by the method.

5 CONCLUSION

In this paper, we presented the method that acquires a vision-motor association for the legged robot which is capable of the vision guided reflective walking. We showed the preliminary experiment and verified that motion patterns can be extracted by the method based on wavelet transform and the centroid method.

We are currently preparing experiment to verify flow pattern categorization. In the future work, we will achieve the navigation based on the vision-motor association for the legged robot.

REFERENCES

[1] H. Kitano, M. Asada, Y. Kuniyoshi, I. Noda, E. Osawa, and H. Matsubara. Robocup: A challeng problem for ai and robotics. In Hiroaki Kitano, editor, *RoboCup-97: Robot Soccer World Cup I*, pp. 1–19. Springer, Lecture Note in Artificail Intelligence 1395, 1998.

[2] S. Uchida, S. Maeyama, A. Ohya, and S. Yuta. Position correction using elevation map for mobile robot on rough terrain. In *Proc. of IEEE/RSJ International Conference on Intelligent Robots and Systems 1998 (IROS '98)*, pp. 582–587, 1998.

[3] C. F. Olson. Subpixel localization and uncertainty estimation using occupancy grids. In *Proc. of IEEE Int. Conf. on Robotics and Automation*, pp. 1987–1992, 1999.

[4] M. Veloso, W. Uther, M. Fujita, M. Asada, and H. Kitano. Playing soccer with legged robots. In *Proc. of IEEE/RSJ International Conference on Intelligent Robots and Systems 1998 (IROS '98)*, pp. 437–442, 1998.

[5] T. Miyashita, K. Hosoda, and M. Asada. Reflective walk based on lifted leg control and vision-cued swaying control. In *Proc. of 1998 BSMEE International Symposium on Climbing and Walking Robots (CLAWAR'98)*, pp. 349–354, 1998.

[6] K. Hosoda, T. Miyashita, S. Takeuchi, and M. Asada. Adaptive visual servoing for legged robots - vision-cued swaying of legged robots in unknown environments-. In *Proc. of the 1997 IEEE/RSJ Int. Conf. on Intelligent Robotics and Systems*, pp. 778–784, 1997.

[7] I. Daubechies. *Ten lectures on wavelets, CBMS-NSF regional conference series in applied mathematics*. Society for Industrial and Applied Mathematics, Philadelphia, 1992.

[8] K. Arikawa and S. Hirose. Development of quadruped walking robot titan-viii. In *Proc. of the 1996 IEEE/RSJ Int. Conf. on Intelligent Robotics and Systems*, pp. 208–214, 1996.

[9] M. Inaba, T. Kamata, and H. Inoue. Rope handling by mobile hand-eye robots. In *Proc. of Int. Conf. on Advanced Robotics*, pp. 121–126, 1993.

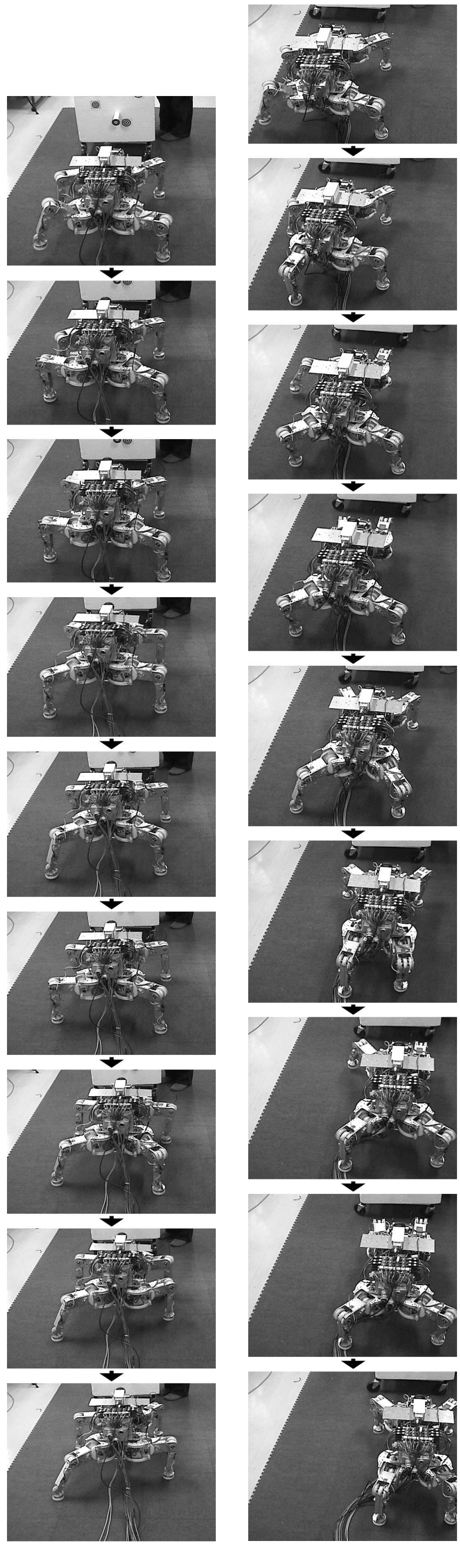

(a) forward motion (b) rightward motion

Figure 8: The reflective walk

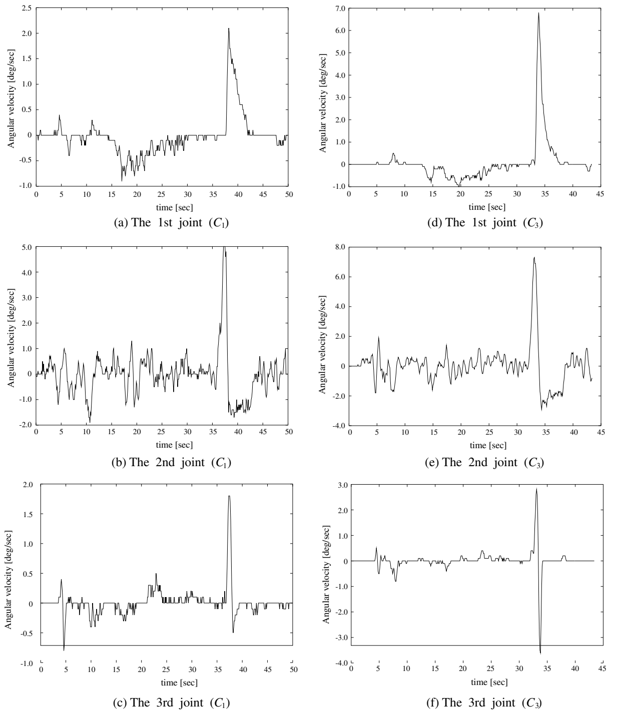

Figure 9: The angular velocities of the right-foreleg during foward motion

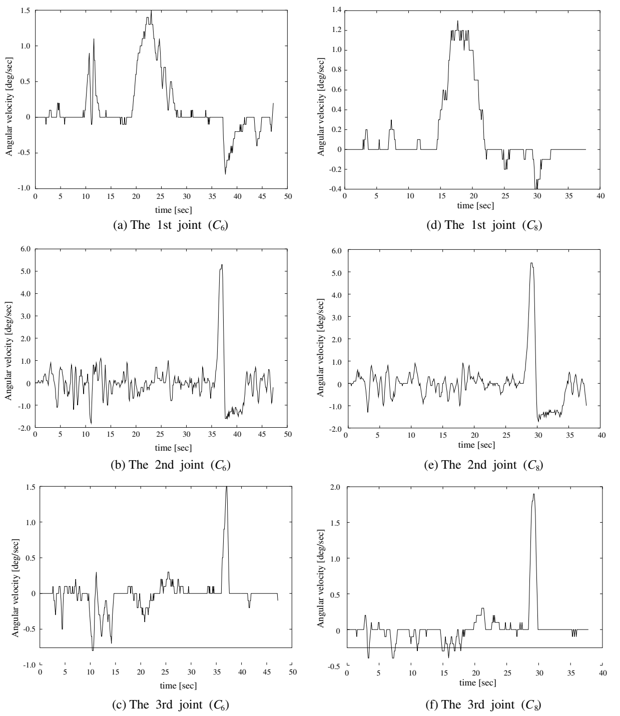

Figure 10: The angular velocities of the right-foreleg during rightward motion

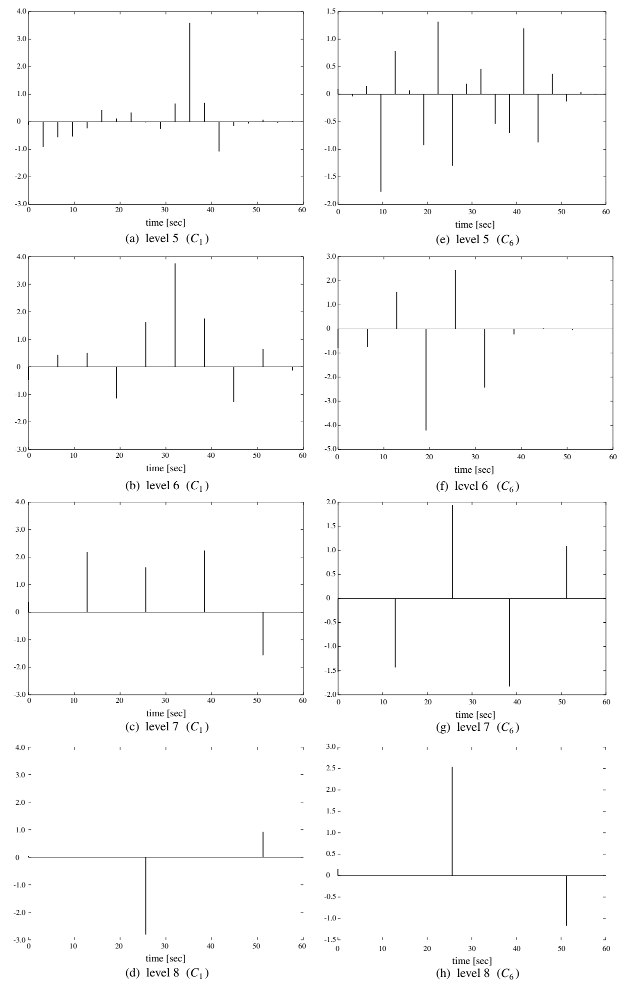

Figure 11: The wavelet coefficients of the first joint angular velocity

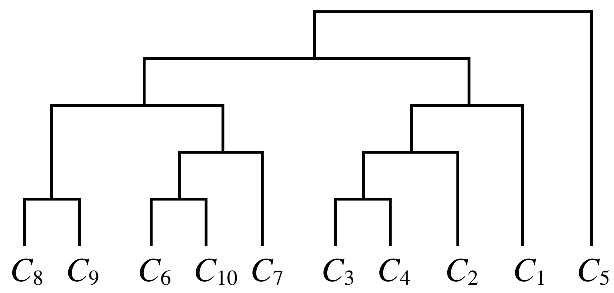

Figure 12: The result of classification